

An Efficient Adaptive Polarimetric Processor with an Embedded CFAR

Hyung-Rae Park, Young-Kil Kwag, and Hong Wang

To improve the detection performance of surveillance radars with polarization diversity, we developed an adaptive polarimetric processor and compared it with other polarimetric processors. We derived our adaptive polarimetric processor, called the polarization discontinuity detector (PDD), from the generalized likelihood ratio (GLR) test principle for the unspecified target component. We derived closed-form expressions of its probabilities of detection and false alarm, and compared its performance to that of the adaptive polarization canceller (APC) and Kelly's GLR processor. The PDD had a performance similar to Kelly's GLR in Gaussian clutter, and both the PDD and Kelly's GLR, which have embedded constant false alarm rates (CFARs), outperformed the APC, especially when the target polarization state was close to the clutter's polarization state. The important difference is that the PDD is much simpler than Kelly's GLR for hardware/software implementation, because the PDD does not require a costly two-parameter filter bank to cover the unknown target polarization state as Kelly's GLR does.

I. Introduction

The use of polarimetric processing techniques for signal detection [1] and parameter estimation [2] is well known, and an excellent tutorial for various radar applications can be found in [3]. For radar target detection in clutter environments, polarimetric processing is a valuable approach, especially when targets are slowly or tangentially moving or Doppler ambiguous [4], [5]. Our investigation aimed to improve detection performance of surveillance radars through adaptive processing of receiver-polarization-diversity data. For this application, both the adaptive polarization canceller (APC) [6] and Kelly's generalized likelihood ratio detector (GLR) [7] can be used. While the APC is much simpler than Kelly's GLR, it suffers from the so-called signal cancellation problem [4] when the target polarization state is close to the clutter's polarization state, since the null depth of the APC is not adjustable. On the other hand, the application of Kelly's GLR for polarimetric processing requires the formation of a two-parameter filter bank to cover the unknown target polarization state, resulting in a significantly increased implementation complexity. The objective of this paper therefore is to develop a well performing, yet sufficiently simple, polarimetric processor for the stated application.

II. Data Model

Consider a radar receiver of two orthogonally polarized channels, i.e., one horizontally (H) polarized and the other vertically (V) polarized. Each channel has its conventional preprocessing and produces an I- and Q-channel output pair, which is sampled for polarimetric processing. Thus, the dual-polarized receiver output can be represented by a sequence of

Manuscript received Oct. 1, 2002; revised Feb. 4, 2003.

Hyung-Rae Park (phone: +82 2 300 0143, e-mail: hrpark@mail.hankong.ac.kr), and Young-Kil Kwag (e-mail: ykkwag@mail.hankong.ac.kr) are with School of Electronics, Telecommunications, and Computer Engineering, Hankuk Aviation University, Goyang-city, Gyeonggi-do, Korea.

Hong Wang (e-mail: hongwang@mailbox.syr.edu) is with Syracuse University, Syracuse, NY 13244-4100, USA.

2×1 complex data vectors, traditionally called range-cell samples. Target signal detection is sought in one range-cell at a time, and the data vector for that range cell is called the primary data vector denoted by \mathbf{x}_p . The secondary data vectors $\mathbf{x}_s(k)$, $k=1,2,\dots,K$ are collected from the adjacent range cells, which are assumed to be free of any target component, and independently and identically distributed.

Under hypothesis H_0 , i.e., the target signal absent hypothesis, the primary data vector \mathbf{x}_p is assumed to be independent of the secondary data vectors, all of which have the same complex Gaussian distribution with a zero mean for the clutter and receiver noise components. The clutter-plus-noise covariance is denoted by

$$\begin{aligned} \mathbf{R} &= E\{\mathbf{x}_s(k)\mathbf{x}_s^H(k)\} \\ &= E\{\mathbf{x}_p\mathbf{x}_p^H|H_0\} \\ &= \sigma_c^2 \begin{bmatrix} 1 & \sqrt{r}\delta \\ \sqrt{r}\delta^* & r \end{bmatrix} + \sigma_n^2 \mathbf{I}, \end{aligned} \quad (1)$$

where δ is seen as the correlation coefficient between H and V channels, r the clutter power ratio of H and V channels, σ_c^2 the H channel clutter power, and σ_n^2 the channel noise power. The superscript H denotes the complex conjugate transpose.

Under H_1 , i.e., the target signal present hypothesis, the primary data vector \mathbf{x}_p is assumed to contain a target component $\mathbf{a} = [a_H \ a_V]^T$, which makes the mean of the primary data become $E\{\mathbf{x}_p\} = \mathbf{a}$. We will derive a new adaptive polarimetric processor by applying the generalized likelihood ratio (GLR) test principle with both the covariance matrix \mathbf{R} and the target component \mathbf{a} being unknown. The resulting processor, called the polarization discontinuity detector (PDD), is thus different from Kelly's GLR processor [7], which is derived under the assumption that the target component is known up to a scalar.

III. Polarization Discontinuity Detector and Its Analytical Performance Expressions

The PDD test statistics, as derived in Appendix A, is given by

$$\eta = \mathbf{x}_p^H \hat{\mathbf{R}}^{-1} \mathbf{x}_p \underset{H_0}{\overset{H_1}{>}} \eta_0, \quad (2)$$

where $\hat{\mathbf{R}} = \sum_{k=1}^K \mathbf{x}_s(k)\mathbf{x}_s^H(k)$ and $0 < \eta_0 < \infty$ is the chosen threshold. The PDD's probabilities of false alarm and detection are derived below. Let $\mathbf{x}_p = \mathbf{R}^{1/2} \mathbf{x}_{p1}$ and

$\mathbf{x}_s(k) = \mathbf{R}^{1/2} \mathbf{x}_{s1}(k)$, $k=1,2,\dots,K$. The test statistic can then be expressed as

$$\begin{aligned} \eta &= \mathbf{x}_{p1}^H \mathbf{R}^{1/2} \hat{\mathbf{R}}^{-1} \mathbf{R}^{1/2} \mathbf{x}_{p1} \\ &= \mathbf{x}_{p1}^H \mathbf{R}^{1/2} \left[\mathbf{R}^{1/2} \left\{ \sum_{k=1}^K \mathbf{x}_{s1}(k)\mathbf{x}_{s1}^H(k) \right\} \mathbf{R}^{1/2} \right]^{-1} \mathbf{R}^{1/2} \mathbf{x}_{p1} \\ &= \mathbf{x}_{p1}^H \left[\sum_{k=1}^K \mathbf{x}_{s1}(k)\mathbf{x}_{s1}^H(k) \right]^{-1} \mathbf{x}_{p1}. \end{aligned} \quad (3)$$

Under H_0 , by the theorem of T^2 statistic [12], the PDD is equivalent to

$$t \underset{H_0}{\overset{H_1}{>}} \eta_0 \tau, \quad (4)$$

where $2t$ has the central χ^2 distribution with the degrees of freedom (df) equal to 4, and 2τ has the central χ^2 distribution with the df equal to $2(K-1)$. Therefore, the probability of false alarm is

$$\begin{aligned} P_F &= P(\eta > \eta_0 | H_0) \\ &= P(t > \eta_0 \tau | H_0) \\ &= \int_0^\infty \left[\int_{\eta_0 \tau}^\infty f_t(t | H_0) dt \right] f_\tau(\tau | H_0) d\tau, \end{aligned} \quad (5)$$

where the probability density functions (pdf) of t and τ are given by

$$f_t(t | H_0) = t \exp(-t) \quad (6)$$

and

$$f_\tau(\tau | H_0) = \frac{\tau^{K-2} \exp(-\tau)}{(K-2)!}. \quad (7)$$

The inner integral of (5) can be completed as

$$\int_{\eta_0 \tau}^\infty f_t(t | H_0) dt = (1 + \eta_0 \tau) \exp(-\eta_0 \tau). \quad (8)$$

Substituting the above into (5) yields

$$P_F = \frac{1 + \eta_0 K}{(1 + \eta_0)^K}. \quad (9)$$

The above expression indicates that the PDD test has a desirable embedded constant false alarm rate (CFAR) feature as P_F does not depend on the clutter-plus-noise covariance matrix.

Under H_1 , $2t$ has a non-central χ^2 distribution with df equal to 4 and non-centrality parameter $2\mu = 2\mathbf{a}^H \mathbf{R}^{-1} \mathbf{a}$. The

pdf of t is thus given by

$$f_t(t|\mathbf{a}, H_1) = \sum_{m=0}^{\infty} \frac{\mu^m}{m!} \exp(-\mu) \frac{t^{m+1}}{(m+1)!} \exp(-t). \quad (10)$$

Since the pdf of the secondary data vectors is the same as under H_0 , the pdf of 2τ remains the same. Thus, the probability of detection given \mathbf{a} is

$$\begin{aligned} P_{D|\mathbf{a}} &= P(t > \eta_0 \tau | \mathbf{a}, H_1) \\ &= \int_0^{\infty} \left[\int_0^{t/\eta_0} f_{\tau}(\tau | H_1) d\tau \right] f_t(t|\mathbf{a}, H_1) dt \\ &= 1 - \int_0^{\infty} \left[\int_{t/\eta_0}^{\infty} f_{\tau}(\tau | H_1) d\tau \right] f_t(t|\mathbf{a}, H_1) dt. \end{aligned} \quad (11)$$

Since the inner integral may be written as

$$\int_{t/\eta_0}^{\infty} f_{\tau}(\tau | H_1) d\tau = \sum_{j=0}^{K-2} \frac{t^{K-2-j} \exp(-t/\eta_0)}{(K-2-j)! \eta_0^{K-2-j}}, \quad (12)$$

substituting the above expression into (11) yields

$$\begin{aligned} P_{D|\mathbf{a}} &= 1 - \sum_{j=0}^{K-2} \frac{\exp(-\mu)}{(K-2-j)!} (1+\eta_0)^{-(K-2-j)} \\ &\quad \times \sum_{m=0}^{\infty} \frac{(K-1-j+m)!}{m!(m+1)!} \mu^m \left(\frac{\eta_0}{1+\eta_0} \right)^{m+2}. \end{aligned} \quad (13)$$

Similar to the finite sum formula [8], the above equation may be expressed as

$$\begin{aligned} P_{D|\mathbf{a}} &= 1 - \eta_0 (1+\eta_0)^{-K} \\ &\quad \times \sum_{j=1}^{K-1} \binom{K}{j+1} \eta_0^j \exp\{-\mu/(1+\eta_0)\} \sum_{m=0}^{j-1} \frac{1}{m!} \{\mu/(1+\eta_0)\}^m. \end{aligned} \quad (14)$$

For the case of a random target polarization, the overall detection probability can be obtained by a statistical average over $\mu = \mathbf{a}^H \mathbf{R}^{-1} \mathbf{a}$. In the following, we model the target polarization state \mathbf{a} by the complex Gaussian with the covariance matrix $\sigma_s^2 \mathbf{I}$. Let $\mathbf{R}^{-1} = \sum_{j=1}^2 \lambda_j \mathbf{v}_j \mathbf{v}_j^H$, where λ_j and \mathbf{v}_j are the j -th eigenvalue and eigenvector of \mathbf{R}^{-1} . Then μ can be expressed as

$$\mu = \lambda_1 |u_1|^2 + \lambda_2 |u_2|^2, \quad (15)$$

where $u_j = \mathbf{v}_j^H \mathbf{a}$. The pdf of μ is given by

$$f_{\mu}(\mu) = \frac{1}{(\lambda_1 - \lambda_2) \sigma_s^2} \left\{ \exp\left(-\frac{\mu}{\lambda_1 \sigma_s^2}\right) - \exp\left(-\frac{\mu}{\lambda_2 \sigma_s^2}\right) \right\}. \quad (16)$$

Therefore, the probability of detection with the above model of the random target polarization state is

$$\begin{aligned} P_D &= \int_0^{\infty} P_{D|\mu} f_{\mu}(\mu) d\mu \\ &= 1 - \frac{\eta_0}{\sigma_s^2 (\lambda_1 - \lambda_2)} (1+\eta_0)^{-K} \\ &\quad \times \sum_{j=1}^{K-1} \binom{K}{j+1} \eta_0^j \sum_{m=0}^{j-1} \left(\frac{1}{1+\eta_0} \right)^m \left(\frac{1}{\gamma_1^{m+1}} - \frac{1}{\gamma_2^{m+1}} \right), \end{aligned} \quad (17)$$

where $\gamma_k = 1/(1+\eta_0) + 1/(\sigma_s^2 \lambda_k)$, $k = 1, 2$.

IV. Detection Performance Comparison

We will compare the detection performance of the APC, PDD, and Kelly's GLR for the case of deterministic target polarization. The exact test statistics of the APC and Kelly's GLR to be used in the comparison are specified in Appendices B and C along with their probabilities of false alarm and detection. Without the loss of generality, we assume the transmitter employs the V channel. The statistical average of the clutter polarization is assumed to be circular with the phase of the H channel leading the phase of the V channel by 90 degrees, i.e., the clutter-plus-noise covariance matrix \mathbf{R} has the form

$$\mathbf{R} = \sigma_c^2 \begin{bmatrix} 1 & |\delta| e^{j\pi/2} \\ |\delta| e^{-j\pi/2} & 1 \end{bmatrix} + \sigma_n^2 \mathbf{I}. \quad (18)$$

Following the definition of the degree of polarization in [9], $|\delta|$ in (18) is the clutter degree of polarization (CDP). With $\delta_n^2 = 1$ for all comparison work in this section, the input clutter-to-noise ratio (CNR_i) is thus equal to σ_c^2 which will be fixed at 30 dB.

For the target polarization state, we choose

$$\mathbf{a} = \xi e^{j\phi} [1 \quad e^{j\phi}]^T, \quad (19)$$

i.e., the case of equal H and V magnitudes. The input signal-to-clutter-plus-noise ratio (SCNR_i) is then

$$\text{SCNR}_i = \frac{\xi^2}{\sigma_c^2 + 1}. \quad (20)$$

The parameter ϕ in (19) adjusts the spherical distance (SD) between the target and clutter on the Poincaré sphere [10], i.e., the separation of the target and clutter in the polarization domain. From (18) and (19) we have $\text{SD} = 90^\circ - \phi$.

The following table shows the four cases of our primary

interest in the performance comparison, classified according to the CDP and SD.

Table 1. Cases for numerical evaluations.

	small SD ($\phi = 85^\circ$)	large SD ($\phi = -60^\circ$)
High CDP ($ \delta = 0.9$)	Case 1	Case 2
Low CDP ($ \delta = 0.3$)	Case 3	Case 4

The performance measure is the probability of detection P_D . In all comparisons, we set the thresholds of the three processors to arrive at the same probability of false alarm of $P_F=10^{-5}$, with the size of the secondary data set $K=20$. As a performance bound, we also include the optimum processor in our comparison, whose test statistic and detection performance are summarized in Appendix D.

Figures 1 and 2 represent the detection performance of Kelly's GLR, the PDD, and the APC for Cases 1 and 2. The PDD and Kelly's GLR outperform the APC significantly in Case 1 where the target and clutter have a similar polarization state, while in Case 2, where the target and clutter are well separated in the polarization domain, there is no significant performance difference.

Figure 3 shows the detection performance when the CDP is low. The performance degradation of the APC is even more significant than that seen in Fig. 1 where the CDP is high.

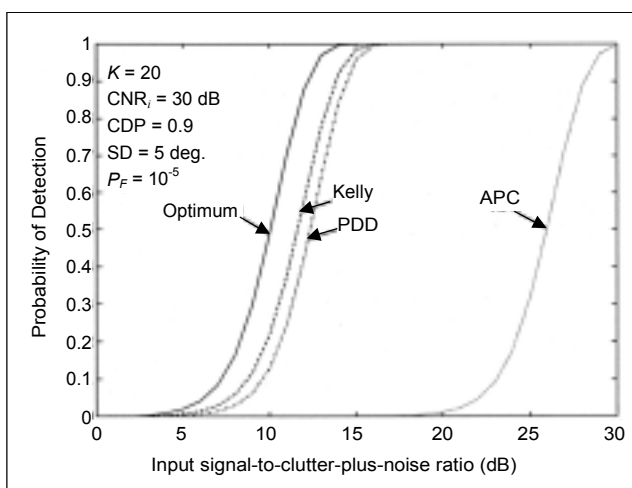


Fig. 1. Performance comparison for Case 1: small spherical distance (SD) and high clutter degree of polarization (CDP).

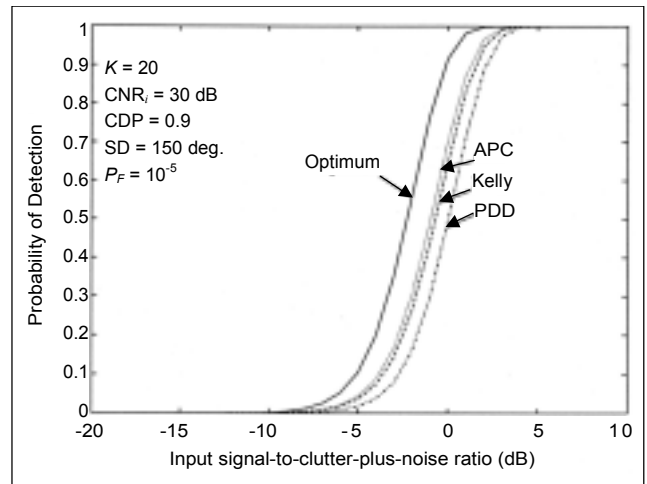


Fig. 2. Performance comparison for Case 2: large SD and high CDP.

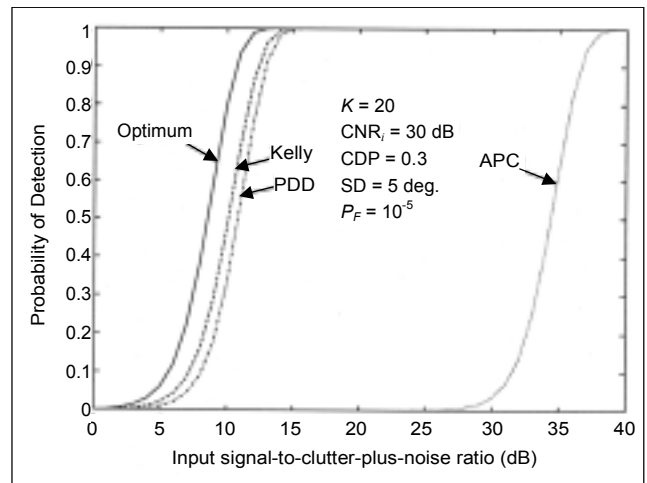


Fig. 3. Performance comparison for Case 3: small SD and low CDP.

As Fig. 4 shows, there is again no significant performance difference among the three processors when the target and clutter are well separated.

The APC's performance degradation with a small target-clutter separation stems from the fact that its clutter suppression is accomplished by nulling, without any adjustment of the null depth. Therefore, it unnecessarily overattenuates a nearby target component, and the problem is more serious when the clutter is less polarized.

In contrast, the PDD and Kelly's GLR are essentially free of this problem.

Both the PDD and Kelly's GLR offer near optimal performance with the latter slightly better than the former, as the latter is assumed to know the target polarization state. However, the implementation of Kelly's GLR is much more costly than that of the PDD. This is because a two-parameter

filter bank on a sufficiently fine grid must be used to cover the actually unknown target polarization state \mathbf{a}_0 for Kelly's GLR in surveillance applications (See Appendix C). For example, if we use a two-dimensional filter bank with a step size of 5° in the angle domain and 0.1 in the amplitude domain, respectively, in (41), the computational complexity of the Kelly's GLR is roughly 720 times larger than that of our PDD processor.

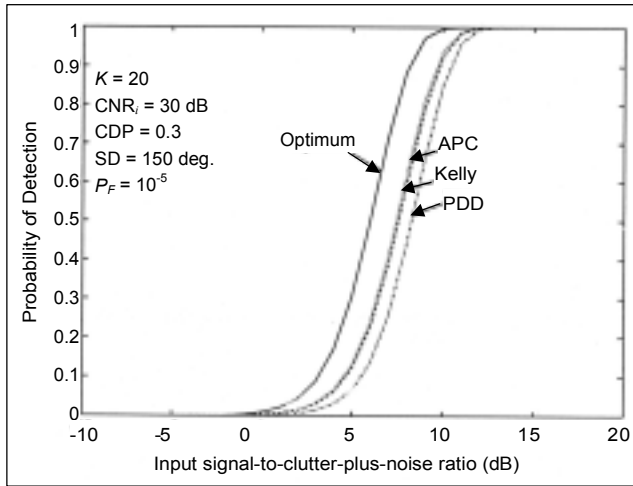


Fig. 4. Performance comparison for Case 4: large SD and low CDP.

Nevertheless, Kelly's GLR has an advantage over the PDD for some applications where the clutter pdf may significantly depart from the assumed Gaussian distribution. As shown in [11], Kelly's GLR is very robust in non-Gaussian interference, and we have not seen this feature with the PDD. Therefore, one should not always prefer the PDD, solely based on its much simpler implementation.

Finally, we like to point out that, because of the performance approximation of the APC as specified in Appendix B, its actual performance is below what is shown in Figs. 1 to 4. In addition, the APC's CFAR performance can be maintained only if K is so large that the APC's weight can be nearly perfectly estimated. Therefore, the PDD is a better choice than the APC for surveillance radar applications.

V. Conclusion

We have shown that our proposed PDD processor has a detection performance very similar to Kelly's GLR in Gaussian clutter, and both the PDD and Kelly's GLR, which have embedded CFARs, outperform the APC, especially when the target polarization state is close to the clutter's polarization state. An important advantage of the PDD over Kelly's GLR is the PDD's low implementation complexity,

as it does not require a two-parameter filter bank to cover the actually unknown target polarization state. The computational complexity of Kelly's GLR is typically a few hundred times larger than that of the PDD processor.

Appendix A: Derivation of the PDD

It is assumed that we obtain a primary data vector \mathbf{x}_p and K secondary data vectors $\mathbf{x}_s(k)$, $k = 1, 2, \dots, K$, by time-filtering a single radar return. Under H_0 , the joint pdf of all data vectors is given by

$$f_0[\mathbf{x}_p, \mathbf{x}_s(1), \mathbf{x}_s(2), \dots, \mathbf{x}_s(K) | H_0] = \left\{ \frac{1}{\pi^2 \|\mathbf{R}\|} \exp[-\text{tr}(\mathbf{R}^{-1} \mathbf{T}_0)] \right\}^{K+1}, \quad (21)$$

where $\|\cdot\|$ and $\text{tr}(\cdot)$ denote the determinant and trace, respectively, and

$$\mathbf{T}_0 = \frac{1}{K+1} (\hat{\mathbf{R}} + \mathbf{x}_p \mathbf{x}_p^H) \quad (22)$$

with $\hat{\mathbf{R}}$ defined by

$$\hat{\mathbf{R}} = \sum_{k=1}^K \mathbf{x}_s(k) \mathbf{x}_s^H(k), \quad (23)$$

which is proportional to the covariance matrix estimate.

Under H_1 , the primary data vector is biased by the presence of an unspecified target polarization vector \mathbf{a} and the joint pdf becomes

$$f_1[\mathbf{x}_p, \mathbf{x}_s(1), \mathbf{x}_s(2), \dots, \mathbf{x}_s(K) | H_1] = \left\{ \frac{1}{\pi^2 \|\mathbf{R}\|} \exp[-\text{tr}(\mathbf{R}^{-1} \mathbf{T}_1)] \right\}^{K+1}, \quad (24)$$

where

$$\mathbf{T}_1 = \frac{1}{K+1} \left\{ \hat{\mathbf{R}} + (\mathbf{x}_p - \mathbf{a})(\mathbf{x}_p - \mathbf{a})^H \right\} \quad (25)$$

By definition of the GLR procedure for the hypothesis test of $H_0: E\{\mathbf{x}_p\} = 0$ vs. $H_1: E\{\mathbf{x}_p\} \neq 0$ [12], we now maximize the above $f_0(\cdot)$ and $f_1(\cdot)$ over the unknown covariance matrix \mathbf{R} and target polarization vector \mathbf{a} . As shown in [12], $f_0(\cdot)$ attains its maximization at $\mathbf{R} = \mathbf{T}_0$ and $f_1(\cdot)$ at $\mathbf{R} = \mathbf{T}_1$ for fixed \mathbf{a} . The resulting maxima are

$$\max_{\mathbf{R}} f_0(\cdot) = \left\{ \frac{1}{(e\pi)^2 \|\mathbf{T}_0\|} \right\}^{K+1} \quad (26)$$

and

$$\max_{\mathbf{R}} f_1(\cdot) = \left\{ \frac{1}{(e\pi)^2 \|\mathbf{T}_1\|} \right\}^{K+1}. \quad (27)$$

Since $f_0(\cdot)$ is not a function of \mathbf{a} and c^{K+1} is a monotonically increasing function for $c \geq 0$, the GLR of $\lambda = \max_{\mathbf{R}, \mathbf{a}} f_1(\cdot) / \max_{\mathbf{R}, \mathbf{a}} f_0(\cdot)$ becomes

$$\lambda = \max_{\mathbf{a}} \left[\frac{\|\mathbf{T}_0\|}{\|\mathbf{T}_1\|} \right] = \frac{\|\mathbf{T}_0\|}{\min_{\mathbf{a}} \|\mathbf{T}_1\|}. \quad (28)$$

Using the determinant equality, we can obtain

$$(K+1)^2 \|\mathbf{T}_0\| = \|\hat{\mathbf{R}}\| (1 + \mathbf{x}_p^H \hat{\mathbf{R}}^{-1} \mathbf{x}_p) \quad (29)$$

$$(K+1)^2 \|\mathbf{T}_1\| = \|\hat{\mathbf{R}}\| \left\{ 1 + (\mathbf{x}_p - \mathbf{a})^H \hat{\mathbf{R}}^{-1} (\mathbf{x}_p - \mathbf{a}) \right\}. \quad (30)$$

Note that $(\mathbf{x}_p - \mathbf{a})^H \hat{\mathbf{R}}^{-1} (\mathbf{x}_p - \mathbf{a})$ of (30) is non-negative definite. Thus, the denominator of (28) becomes minimal when $\mathbf{x}_p = \mathbf{a}$ as seen in (30). Thus, (28) becomes

$$\lambda = 1 + \mathbf{x}_p^H \hat{\mathbf{R}}^{-1} \mathbf{x}_p \underset{H_0}{\overset{H_1}{>}} \lambda_0. \quad (31)$$

Finally, the GLR decision rule $\lambda \underset{H_0}{\overset{H_1}{>}} \lambda_0$ is obviously equivalent to

$$\eta = \mathbf{x}_p^H \hat{\mathbf{R}}^{-1} \mathbf{x}_p \underset{H_0}{\overset{H_1}{>}} \eta_0 \quad (32)$$

with $\eta_0 = \lambda_0 - 1$.

Appendix B: Adaptive Polarization Canceller-Based Detector (APC) and Its Detection Performance

This appendix specifies the test statistic of the adaptive polarization canceller [6] followed by a Cell Averaging-CFAR processor. The canceller coefficient $\hat{\mathbf{w}} = [\hat{w}_H \ \hat{w}_V]^T$ is obtained from the clutter-plus-noise covariance matrix estimate as

$$\hat{w}_H = 1$$

$$\hat{w}_V = - \left\{ 1 + \frac{(\hat{r}_{HH} - \hat{r}_{VV})^2 + (\hat{r}_{HH} - \hat{r}_{VV}) \sqrt{(\hat{r}_{HH} - \hat{r}_{VV})^2 + 4|\hat{r}_{HV}|^2}}{2|\hat{r}_{HV}|^2} \right\}^{1/2} \times \exp\{-j \arg(\hat{r}_{HV})\}, \quad (33)$$

where $\hat{r}(\cdot)$ is defined by

$$\hat{\mathbf{R}}_K = \frac{1}{K} \sum_{k=1}^K \mathbf{x}_s(k) \mathbf{x}_s^H(k) = \begin{bmatrix} \hat{r}_{HH} & \hat{r}_{HV} \\ \hat{r}_{VH} & \hat{r}_{VV} \end{bmatrix}. \quad (34)$$

The output of the canceller is

$$z_p = \hat{\mathbf{w}}^H \mathbf{x}_p$$

$$z_s(k) = \hat{\mathbf{w}}^H \mathbf{x}_s(k), \quad k = 1, 2, \dots, K. \quad (35)$$

The decision rule with the Cell Averaging-CFAR detector is then

$$\eta = \frac{|z_p|^2}{\sum_{k=1}^K |z_s(k)|^2} \underset{H_0}{\overset{H_1}{>}} \eta_0. \quad (36)$$

Obviously, $\hat{\mathbf{w}}$ is a random variable depending on the secondary data $\mathbf{x}_s(k)$, $k = 1, 2, \dots, K$, which makes the detection performance difficult to derive. However, for large secondary data sets, for example, $K \geq 20$, $\hat{\mathbf{w}}$ should have little randomness, especially with highly polarized clutter. Thus, we will approximate $\hat{\mathbf{w}}$ with the canceller coefficient from the true covariance matrix in the detection performance comparison of this paper. With this approximation, the detection performance for the deterministic target can be easily found as

$$P_F = (1 + \eta_0)^{-K} \quad (37)$$

and

$$P_{D|a} = 1 - (1 + \eta_0)^{-K} \sum_{j=1}^K \binom{K}{j} \eta_0^j \exp\{-\beta / (1 + \eta_0)\} \times \sum_{m=0}^{j-1} \frac{1}{m!} \{\beta / (1 + \eta_0)\}^m, \quad (38)$$

where

$$\beta = \frac{\mathbf{w}^H \mathbf{a} \mathbf{a}^H \mathbf{w}}{\mathbf{w}^H \mathbf{R} \mathbf{w}}. \quad (39)$$

Appendix C: Kelly's GLR as a Polarimetric Processor

Kelly's GLR [7] can be applied to the polarization domain with its steering vector being replaced by the expected target polarization state. It should be noted that Kelly's GLR is for

the hypothesis test of $H_0 : E\{\mathbf{x}_p\} = 0$ vs. $H_1 : E\{\mathbf{x}_p\} = \mathbf{a}$ prespecified target polarization state (up to an unspecified deterministic scalar). We select this processor in our comparison as it possesses good detection performance with an embedded CFAR feature.

Following [7], the test statistic of Kelly's GLR is

$$\eta = \frac{|\mathbf{a}_0^H \hat{\mathbf{R}}^{-1} \mathbf{x}_p|^2}{\mathbf{a}_0^H \hat{\mathbf{R}}^{-1} \mathbf{a}_0 (1 + \mathbf{x}_p^H \hat{\mathbf{R}}^{-1} \mathbf{x}_p)} \underset{H_0}{\overset{H_1}{>}} \eta_0, \quad (40)$$

where the "steering" vector \mathbf{a}_0 is specified as

$$\mathbf{a}_0 = [1 \quad \alpha e^{j\phi}]^T. \quad (41)$$

The above form of \mathbf{a}_0 implies that two parameters, α and ϕ , are required to set up the "filter" bank when the target polarization state is unknown. This is in contrast to the applications of Kelly's GLR in the spatial or Doppler domain, where only a single parameter is required to set up the filter bank.

The probability of false alarm of Kelly's GLR is independent of the clutter-plus-noise covariance matrix and given by

$$P_F = (1 - \eta_0)^{K-1}. \quad (42)$$

Following [7], the probability of detection for the deterministic target of $\mathbf{a} = \xi \mathbf{a}_0 = \xi [1 \quad \alpha e^{j\phi}]^T$ is

$$P_{D|\rho, \mathbf{a}} = 1 - (1 - \eta_0)^{K-1} \times \sum_{j=1}^{K-1} \binom{K-1}{j} \left(\frac{\eta_0}{1 - \eta_0} \right)^j \exp\{-\rho\beta(1 - \eta_0)\} \times \sum_{m=0}^{j-1} \frac{\{\rho\beta(1 - \eta_0)\}^m}{m!}, \quad (43)$$

where $\beta = \xi^2 \mathbf{a}_0^H \mathbf{R}^{-1} \mathbf{a}_0$ with ξ being a positive constant representing the target magnitude in the reference H channel and the pdf of ρ given by

$$f_\rho(\rho) = K\rho^{K-1}. \quad (44)$$

Appendix D: Optimum Processor and Its Performance

For convenience of reference, we summarize below the results on the optimum processor, which assumes that the covariance matrix \mathbf{R} is known and that the target polarization

state is known up to a deterministic scalar. The test statistic of the optimum processor is

$$\eta = \frac{|\mathbf{a}_0^H \mathbf{R}^{-1} \mathbf{x}_p|^2}{\mathbf{a}_0^H \mathbf{R}^{-1} \mathbf{a}_0} \underset{H_0}{\overset{H_1}{>}} \eta_0, \quad (45)$$

where $\mathbf{a}_0^H \mathbf{R}^{-1} \mathbf{a}_0$ is selected for the denominator to achieve CFAR. Under H_0 , 2η has the central χ^2 distribution with the df equal to 2 and the pdf of η is

$$f_\eta(\eta|H_0) = \exp(-\eta). \quad (46)$$

The probability of false alarm is then

$$P_F = \exp(-\eta_0). \quad (47)$$

Under H_1 , 2η has the non-central χ^2 distribution with the df equal to 2 and the non-centrality parameter $2\mu = 2\xi^2 \mathbf{a}_0^H \mathbf{R}^{-1} \mathbf{a}_0$ and $\mathbf{a} = \xi \mathbf{a}_0$. The pdf of η is thus given by

$$f_\eta(\eta|\gamma, H_1) = \sum_{m=0}^{\infty} \frac{\mu^m}{m!} \exp(-\mu) \frac{\eta^m}{m!} \exp(-\eta), \quad (48)$$

and the probability of detection conditioned on ξ is

$$P_{D|\xi} = \int_{\eta_0}^{\infty} \exp\{-(\eta + \mu)\} \sum_{m=0}^{\infty} \frac{1}{m!m!} \eta^m \mu^m d\eta = 1 - \exp(-\mu) \int_0^{\eta_0} \exp(-t) I_0(2\sqrt{\mu t}) dt. \quad (49)$$

References

- [1] V.C. Vannicola and S. Lis, "Polarization Vector Signal Processing for Radar Clutter Suppression," *Inverse Methods in Electromagnetic Imaging, Part 2; NATO ASI Series C: Mathematical and Physical Sciences*, vol. 143, 1983, pp. 739-770.
- [2] J. Li and R.T. Compton Jr., "Angle and Polarization Estimation in a Coherent Signal Environment," *IEEE Trans. on Aeros. and Electr. Sys.*, vol. AES-29, no. 3, July 1993, pp. 706-716.
- [3] D. Giuli, "Polarization Diversity in Radars," *Proc. of IEEE*, vol. 74, no. 2, Feb. 1986, pp. 245-269.
- [4] M. Wicks et al., "Polarization Radar Processing Technology," *Proc. IEEE 1990 Int'l Radar Conf.*, Arlington, VA, May 7-9, 1990, pp. 409-416.
- [5] H.R. Park, J. Li, and H. Wang, "Polarization-Space-Time Domain Generalized Likelihood Ratio Detection of Radar Targets," *Signal Processing (Elsevier)*, vol. 41, 1995, pp.153-164.
- [6] M. Gherardelli, D. Giuli, and M. Fossi, "Suboptimum Adaptive Polarization Cancellers for Dual-Polarization Radars," *IEE Proc.*, vol. 135, Pt. F, no. 1, Feb. 1988, pp. 60-72.
- [7] E.J. Kelly, "An Adaptive Detection Algorithm," *IEEE Trans. on Aeros. and Electr. Sys.*, vol. AES-22, no. 1, Mar. 1986, pp. 115-127.

- [8] E.J. Kelly, "Finite-Sum Expressions for Signal Detection Probabilities," *Tech. report 566*, M.I.T. Lincoln Lab, 1981.
- [9] W.M. Boerner et al., *Direct and inverse methods in radar polarimetry, Pt. I and II, NATO ASI Series C*, vol. 350, 1988.
- [10] G.A. Deschamps and P.E. Mast, "Poincaré Sphere Representation of Partially Polarized Field," *IEEE Trans. on Ant. and Propa.*, vol. AP-21, no. 4, July 1973, pp. 474-478.
- [11] L. Cai and H. Wang, "Performance comparisons of the modified SMI and GLR algorithms," *IEEE Trans. on Aeros. and Electr. Sys.*, vol. AES-27, no. 3, May 1991, pp. 487-491.
- [12] T.W. Anderson, *An Introduction to Multivariate Statistical Analysis*, John Wiley & Sons, 1971.
- [13] C.J. Kim, "Performance Analysis of the Clutter map CFAR Detector with Noncoherent Integration," *ETRI J.*, vol. 15, no. 2, Oct. 1993, pp. 1-9.



Hong Wang received the PhD degree in electrical engineering from the University of Minnesota in Minneapolis, USA, in 1985. He joined the Faculty of the Department of Electrical and Computer Engineering at Syracuse University in Syracuse, NY, USA, in 1985, where he is currently a Professor. He has been a consultant to Technology Service Corporation, Kaman Science Corporation, Southeastern Center for Electrical Engineering Education, and the Rome Air Development Center. His research interest is signal processing with its application to radar and IR systems. Dr. Wang is the recipient of the 1988 IEEE Acoustics, Speech, and Signal Processing Society's Paper Award.



Hyung-Rae Park received the BS degree from Hankuk Aviation University, Korea, MS degree from Yonsei University, Korea, and PhD degree from Syracuse University in the USA, all in Electrical Engineering in 1982, 1985, and 1993. From 1985 to 1999, he worked for ETRI in Korea as a Principal Researcher and the Section

Head in the Mobile Communication Research Division. From 1999 to 2000, he was Vice President of C&S Technology, Inc. in Korea. Currently, he is a Faculty Member of the School of Electronics, Telecommunications, and Computer Engineering, Hankuk Aviation University in Korea. His research interests are in the areas of CDMA algorithm development, smart antenna, space-time coding, 4G system design, and radar signal processing.



Young-Kil Kwag received the BS degree from National Aviation University in 1976, MS degree from Korea Advanced Institute of Science and Technology in 1981, and PhD degree from Ohio University in Ohio, USA, in 1987. From March 1976 to March 2001, he worked with the Agency for Defense

Development (ADD) as a Principal Researcher and the Research Division Head in the areas of radar systems and radar signal processing, spaceborne synthetic aperture radar systems. He was an Adjunct Professor at KAIST from 1992 to 1993. He was a program manager at the Matra Marconi Space in the UK for the Spaceborne SAR Program from 1997 to 1999. Since March 2001, he has been a Faculty Member in the School of Electronics, Telecomm, and Computer Eng., and the Director of Aerospace and Aviation Electronics Research Center, Hankuk Aviation University in Seoul, Korea. His research interests include radar and adaptive signal processing, spaceborne SAR system and SAR image processing, aeronautical communications and surveillance radar, data link, avionics-CNS/ATM, and DSP applications to radar and communications.